Cell Research (2014) 24:870-885.

www.nature.com/cr

ORIGINAL ARTICLE

Trypanosoma brucei TIF2 suppresses *VSG* switching by maintaining subtelomere integrity

Sanaa E Jehi[1], Fan Wu[1], Bibo Li[1, 2, 3, 4]

[1]*Department of Biological, Geological, and Environmental Sciences, Center for Gene Regulation in Health and Disease, Cleveland State University, Cleveland, OH 44115, USA;* [2]*The Rockefeller University, New York, NY 10065, USA;* [3]*Department of Molecular Genetics, Cleveland Clinic Lerner Research Institute, Cleveland, OH 44195, USA;* [4]*Case Comprehensive Cancer Center, Case Western Reserve University, Cleveland, OH 44106, USA*

Subtelomeres consist of sequences adjacent to telomeres and contain genes involved in important cellular functions, as subtelomere instability is associated with several human diseases. Balancing between subtelomere stability and plasticity is particularly important for *Trypanosoma brucei*, a protozoan parasite that causes human African trypanosomiasis. *T. brucei* regularly switches its major variant surface antigen, variant surface glycoprotein (VSG), to evade the host immune response, and VSGs are expressed exclusively from subtelomeres in a strictly monoallelic fashion. Telomere proteins are important for protecting chromosome ends from illegitimate DNA processes. However, whether they contribute to subtelomere integrity and stability has not been well studied. We have identified a novel *T. brucei* telomere protein, *T. brucei* TRF-Interacting Factor 2 (*Tb*TIF2), as a functional homolog of mammalian TIN2. A transient depletion of *Tb*TIF2 led to an elevated *VSG* switching frequency and an increased amount of DNA double-strand breaks (DSBs) in both active and silent subtelomeric bloodstream form expression sites (BESs). Therefore, *Tb*TIF2 plays an important role in *VSG* switching regulation and is important for subtelomere integrity and stability. *Tb*TIF2 depletion increased the association of *Tb*RAD51 with the telomeric and subtelomeric chromatin, and *Tb*RAD51 deletion further increased subtelomeric DSBs in *Tb*TIF2-depleted cells, suggesting that *Tb*RAD51-mediated DSB repair is the underlying mechanism of subsequent *VSG* switching. Surprisingly, significantly more *Tb*RAD51 associated with the active BES than with the silent BESs upon *Tb*TIF2 depletion, and *Tb*RAD51 deletion induced much more DSBs in the active BES than in the silent BESs in *Tb*TIF2-depleted cells, suggesting that *Tb*RAD51 preferentially repairs DSBs in the active BES.

***Keywords*:** subtelomere; telomere; *Trypanosoma brucei; VSG* switching; RAD51; antigenic variation

Cell Research (2014) **24**:870-885. doi:10.1038/cr.2014.60; published online 9 May 2014

Introduction

The ends of linear chromosomes form specialized nucleoprotein complexes termed telomeres, which often consist of simple repetitive TG-rich sequences (e.g., $(TTAGGG)_n$ in vertebrates and *Trypanosoma brucei*) and associated proteins. Sequences located next to telomeres are subtelomeres. In contrast to previous beliefs that subtelomeres are barren regions of no importance, they contain genes involved in important cellular functions, and instability of human subtelomere regions is often associated with diseases. For example, the *double homeobox 4* (*DUX4*) gene locates in the D4Z4 repeat array at human 4q35 subtelomere [1]. Drastically reduced D4Z4 repeat number can lead to abnormal *DUX4* transcription and is associated with facioscapulohumeral muscular dystrophy (FSHD) [2]. Submicroscopic deletion of subtelomeric 6p25 and 9q has been recognized as clinically identifiable syndromes [3, 4]. In addition, some *OR* genes encoding olfactory receptors are located at subtelomeres, and changes in subtelomeres contribute to the diversity of the *OR* gene family [5].

Subtelomeres are particularly important for a number

Correspondence: Bibo Li
Tel: +1 216 687-2444
E-mail: b.li37@csuohio.edu
Received 27 November 2013; revised 11 March 2014; accepted 7 April 2014; published online 9 May 2014

of microbial pathogens that undergo antigenic variation, including *T. brucei* that causes human African trypanosomiasis, *Plasmodium falciparum* that causes malaria, *Pneumocystis jirovecii* that causes pneumonia, and *Borrelia burgdorferi* that causes Lyme disease [6]. These pathogens regularly switch their major surface antigen to evade the host immune response, and genes encoding variant surface antigens are expressed exclusively (or sometimes in *P. falciparum*) from subtelomeric regions in a strictly monoallelic fashion [6]. Therefore, plasticity at subtelomeric regions is necessary for these microbial pathogens. However, maintaining a relatively stable subtelomere is also important, as unstable subtelomeres can lead to loss of functional surface antigen genes. How do these pathogens maintain a delicate balance between stability and plasticity at their subtelomeres is not well known.

Maintenance of subtelomere stability is challenging because subtelomeres often consist of DNA blocks duplicated on multiple chromosomes and are highly dynamic with very heterogeneous sequences, sizes, and copy numbers [7]. Human subtelomeres are hot spots of interchromosomal recombination and segmental duplications [8]. A high level of nucleotide divergence among *Saccharomyces* yeasts has been observed at the subtelomeres [9]. Similarly in *T. brucei,* subtelomeres have been considered fragile sites and undergo DNA recombination frequently [10].

It is well known that proteins associated with the telomere are essential for maintaining the telomere stability [11]. However, whether telomere proteins directly contribute to subtelomere stability has not been well studied. "Shelterin" is a six-member complex that associates with the vertebrate telomere [12]. In the complex, TRF1 and TRF2 bind the duplex TTAGGG repeats [13-15], and the TPP1/POT1 heterodimer binds the telomeric single-stranded 3′ overhang [16]. As a core component of Shelterin, TIN2 interacts with TRF1, TRF2, and TPP1 directly [17-21]. Shelterin components are essential for preventing the natural chromosome ends from being processed as double-strand breaks (DSBs) [12]. For example, TRF2 suppresses ATM activation and POT1 inhibits ATR activation at the telomere [22]. In addition, telomere proteins are important for telomeric DNA replication. Deletion of TRF1 results in replication fork stalling in telomere repeats and fragile telomeres [23], and TRF2 coordinates with its interacting factor Apollo, a 5′ exonuclease, to relieve topological stress during telomere replication [24]. *X. laevis* TRF2 and fission yeast TAZ1 that binds the duplex telomere DNA are also required for DNA replication at the telomere [25, 26]. Mammalian TIN2 also interacts directly with SA1, a telomere-specific cohesin subunit [27, 28], and HP1γ [29], which is required to establish/maintain telomere cohesion and maintain proper telomere length [29]. Presumably, replication stress or improper sister telomere pairing resulting from dysfunctional telomere proteins can affect subtelomere stability, but this has not been shown in microbial pathogens such as *T. brucei*.

T. brucei is the causal agent of human African trypanosomiasis, which is fatal without treatment. Bloodstream form (BF) *T. brucei* stays in extracellular spaces inside the mammalian host and regularly switches its major surface antigen, variant surface glycoprotein (VSG), to evade the host immune response [30]. *T. brucei* has more than 2 000 *VSG* genes and pseudogenes [31], but VSGs are exclusively expressed from BF expression sites (BESs), which are polycistronic transcription units at subtelomeres [32]. *VSG* is the last gene in any BES, located less than 2 kb from the telomere and 40-60 kb downstream of the BES promoter [33]. *T. brucei* has multiple BESs (15-20 in the lister 427 strain used in this work), but only one is fully active, expressing a single type of VSG at any time [34, 35].

VSG switching has several major pathways [36]. In *in situ* switching, an originally silent BES is expressed, while the originally active BES is silenced without DNA rearrangements. Other major *VSG* switching pathways are homologous recombination (HR) mediated. In crossover (CO) events, part of the active BES, including the *VSG* gene, changes place with that of a silent BES without losing any genetic information. In gene conversion (GC) events, a silent *VSG* is copied into the active BES to replace the active *VSG* gene, resulting in the loss of the originally active *VSG* and duplication of the newly active *VSG*. GC is the preferred mechanism of *VSG* switching [36]. It can encompass only the *VSG* gene and its neighboring regions (*VSG* GC) or the entire BES (ES GC). Several proteins play important roles in *VSG* switching. RAD51 binds to the single-stranded 3′ overhang at DNA DSBs following 5′ resection and promotes strand invasion during HR [37]. Deletion of *Tb*RAD51 or *Tb*RAD51-3 leads to decreased *VSG* switching frequencies [38, 39]. *Tb*BRCA2 is similarly required for efficient *VSG* switching [40]. In contrast, deletion of TOPO3 and RMI1 leads to more frequent *VSG* switching [41, 42]. Recent studies showed that inducing DSBs in the active BES increases the *VSG* switching rate, and different *VSG* switching mechanisms are used depending on the DSB position [10, 43]. As high as 25% of DSBs downstream of the active *VSG* result in the loss of the entire active BES [10], and an accompanying *in situ* switch can give rise to ES loss coupled with *in situ* switchers (ES loss + *in situ*). Interestingly, DSBs in silent BESs seldom lead

to *VSG* switching [10]. However, how DSBs in the active and silent BESs lead to different outcomes is not well known.

T. brucei is transmitted by the tsetse fly (*Glossina spp.*). In the midgut of the insect host, procyclic form (PF) *T. brucei* expresses procyclins instead of VSG. Upon reaching the salivary glands, *T. brucei* differentiates into the metacyclic form, reacquires infectivity, and expresses metacyclic VSGs (mVSGs) from metacyclic ESs (MESs), which are monocistronic transcription units located in subtelomeric regions [44]. *mVSGs* are silenced soon after *T. brucei* cells are transmitted into the mammalian host.

We have shown that a telomere protein, *Tb*RAP1, plays an essential role in silencing subtelomeric *VSGs* [45, 46]. However, it is not known whether telomere proteins influence *VSG* switching, although extremely short telomeres (~1.5 kb) elevate *VSG* switching frequencies by ~10-fold [47]. In this study, we identified a novel *T. brucei* telomere protein, *T. brucei* TRF-Interacting Factor 2 (*Tb*TIF2), that interacts with *Tb*TRF and is functionally homologous to mammalian TIN2. A transient depletion of *Tb*TIF2 by RNAi led to an increase in *VSG* switching frequency where most switchers arose from GC events, indicating that telomere proteins are indeed important for *VSG* switching regulation and contribute to subtelomere stability. Depletion of *Tb*TIF2 increased subtelomeric DSBs, indicating that *Tb*TIF2 contributes directly to subtelomere integrity. More *Tb*RAD51 associated with telomeric and subtelomeric chromatin following *Tb*TIF2 depletion, and this increase was, surprisingly, much stronger at the active BES than at silent ones. Deletion of *Tb*RAD51 further increased subtelomeric DSB levels in *Tb*TIF2-depleted cells, particularly in the active BES, suggesting that *Tb*RAD51-mediated DSB repair in the active BES is the underlying mechanism of the increased *VSG* switching and that the choice of DSB repair mechanisms may be influenced by transcriptional status of the DSB site.

Results

T. brucei TIF2 is a telomeric protein

We have previously identified *T. brucei* TRF as a telomere-binding protein [48]. We have also identified *Tb*RAP1 as a *Tb*TRF-interacting factor and have shown that *Tb*RAP1 is essential for silencing of subtelomeric BES-linked and metacyclic *VSG* genes [45, 46]. To further investigate telomere functions in antigenic variation, we attempted to identify additional *Tb*TRF-interacting factors.

In order to pull down the *Tb*TRF protein complex specifically, we established a *Tb*TRF single-allele knockout PF strain with the remaining endogenous *Tb*TRF allele tagged with an N-terminal FLAG-HA-HA (F2H) epitope. This strain grows normally (Supplementary information, Figure S1A), indicating that the sole F2H-*Tb*TRF allele is functional. We immunoprecipitated (IP) the whole cell extract with the FLAG monoclonal antibody M2 (Sigma), eluted the IP product with the FLAG peptide, and immunoprecipitated the eluate with the HA monoclonal antibody 12CA5 (MSKCC monoclonal AB core). The final IP product was separated on a polyacrylamide gel (Supplementary information, Figure S1B) and analyzed by mass spectrometry. WT cells without the F2H tag were treated exactly the same way and proteins identified in the final IP product by mass spectrometry were considered as background contaminants. In addition to *Tb*TRF, we identified a novel protein (TriTrypDB ID: *Tb*427.03.1560) in the *Tb*TRF IP product.

To verify the interaction between *Tb*427.03.1560 and *Tb*TRF, we first performed yeast two-hybrid analysis. Full-length *Tb*427.03.1560 and *Tb*TRF interact much more strongly than *Tb*TRF homodimerization (Figure 1A and Supplementary information, Figure S1C), confirming that *Tb*427.03.1560 interacts with *Tb*TRF directly when analyzed in yeast. We therefore named this protein *T. brucei* TRF-Interacting Factor 2 (*Tb*TIF2; *Tb*RAP1 is *Tb*TRF-interacting factor 1 [45]). Sequence analysis of *Tb*TIF2 did not identify any functional domains. However, alignment of *Tb*TIF2 with known telomere proteins showed that it is weakly homologous to TIN2 (14% sequence identity between *Tb*TIF2 and human TIN2; Supplementary information, Figure S1D). *T. brucei* telomere proteins exhibit significant similarities to their vertebrate homologs only within functional domains. The identity between *Tb*TRF and vertebrate TRFs is 18%-22% in the Myb domain and 9%-12% in the TRFH domain, respectively [48]. The identity between *Tb*RAP1 and vertebrate RAP1s is 8%-23% within various functional domains [45]. In addition, yeast two-hybrid analysis using various fragments of *Tb*TIF2 and *Tb*TRF showed that the N-terminal half of *Tb*TIF2 interacts with the TRFH domain of *Tb*TRF (Figure 1A), which is partially conserved with the situation in mammalian cells, where the N-terminal half of TIN2 interacts with a short peptide in the linker region of TRF2, while a short stretch towards the C-terminal half of TIN2 interacts with the TRFH domain of TRF1 [49]. Therefore, *Tb*TIF2 is likely a functional homolog of vertebrate TIN2.

To further characterize *Tb*TIF2, we established *T. brucei* strains that carry a C-terminally F2H-tagged *Tb*TIF2 at its endogenous locus and found that *Tb*TIF2 and *Tb*TRF co-immunoprecipitated in both BF (Figure 1B) and PF (Supplementary information, Figure S1E) cells when

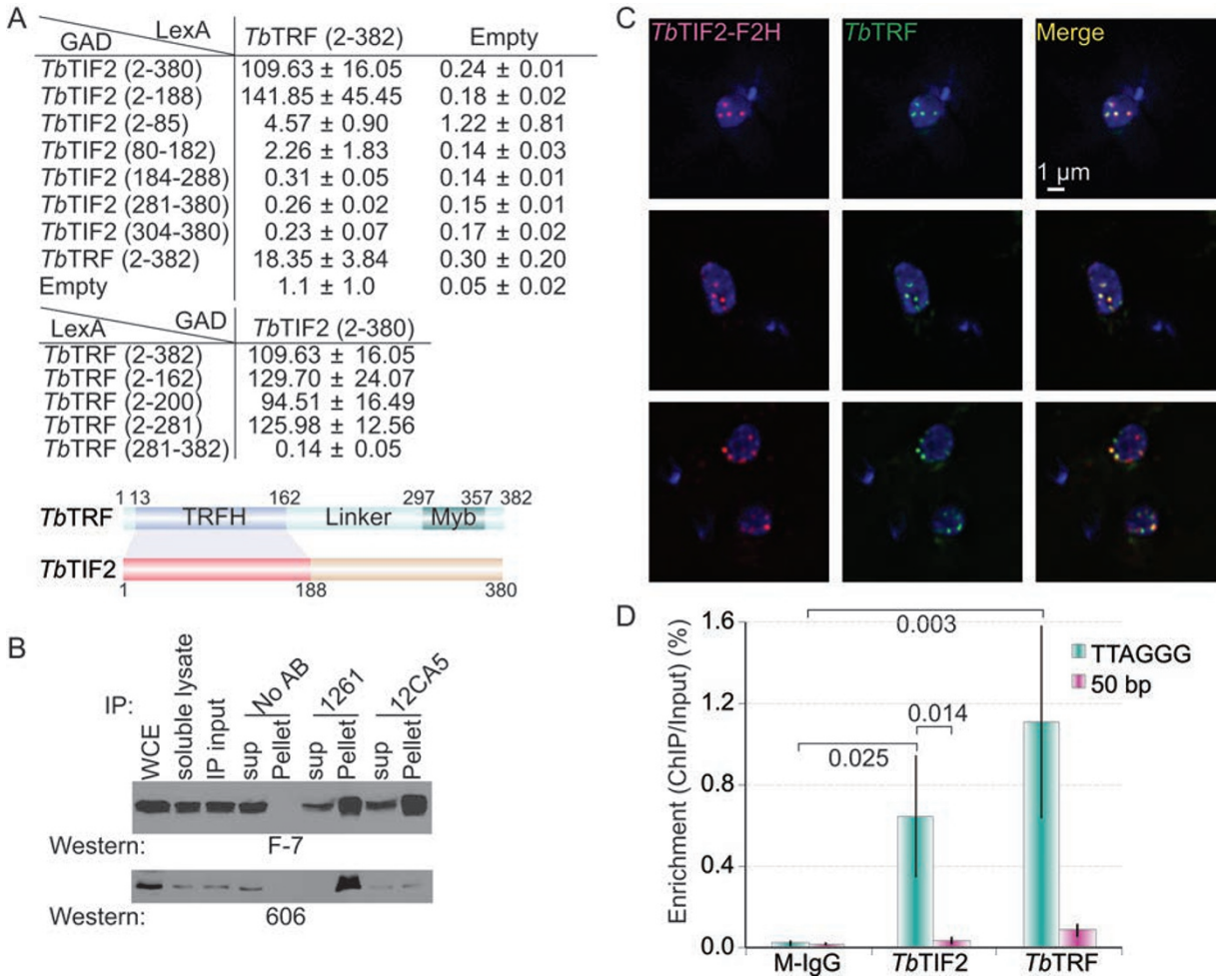

Figure 1 *Tb*TIF2 interacts with *Tb*TRF and associates with telomeres. **(A)** *Tb*TIF2 and *Tb*TRF interact in yeast two-hybrid analysis. Top, different Gal4 Activation Domain (GAD)-fused *Tb*TIF2 fragments (starting and ending amino acids of each fragment are listed in the parentheses) were tested for their interaction with LexA-fused full-length *Tb*TRF or just LexA (empty). The expression of GAD-*Tb*TIF2 fragments was examined by western blotting (Supplementary information, Figure S1C). Middle, different LexA-fused *Tb*TRF fragments were tested for their interaction with the GAD-fused full-length *Tb*TIF2. Control experiments testing the interaction between LexA-*Tb*TRF and GAD alone were performed previously [48]. β-galactosidase activities, shown as average (calculated from at lease four independent tests) ± standard deviations, reflect the expression of the reporter *LacZ* gene resulting from the interaction between the LexA- and GAD-fused proteins. A summary of the interaction between *Tb*TIF2 and *Tb*TRF is shown at the bottom. **(B)** *Tb*TIF2 and *Tb*TRF interact *in vivo*. Whole Cell Extract (WCE) was prepared from SM/*Tb*TIF2-F2H. The soluble fraction of the lysate (soluble lysate) was cleared with protein G beads (IP input) and Immunoprecipitated with *Tb*TRF antibody 1261 [48], HA antibody 12CA5, or no antibody. IP supernatant (sup) and IP product (pellet) were subsequently analyzed by western blotting using HA antibody F-7 (Santa Cruz Biotechnology, Inc.) or chicken anti-*Tb*TRF antibody 606 [45]. **(C)** Immunofluorescence analysis of SM/*Tb*TIF-F2H cells using 12CA5 and 1261. DAPI stains DNA in both the nucleus (larger blue circle) and the kinetoplast (small blue dot). **(D)** ChIP analysis in SM/*Tb*TIF2-F2H cells using F-7, 1261, or mouse IgG (M-IgG). ChIP products were hybridized with a TTAGGG or a 50 bp repeat probe. Representative slot blots are shown in Supplementary information, Figure S1F. The blots were exposed to a phosphorimager and results were quantified by ImageQuant. Average was calculated from at least three independent experiments. In this and following figures, error bars represent standard deviation. Numbers next to the brackets indicate *P*-values (unpaired *t*-tests) between different experiments. $P < 0.05$ is considered to be significant.

we used either *Tb*TRF antibody or HA antibody for IP, further confirming that *Tb*TIF2 and *Tb*TRF interact *in vivo*.

Immunofluorescence using an HA antibody and a *Tb*TRF antibody (served as a marker for the telomere) in *Tb*TIF2-F2H-containing cells showed that *Tb*TIF2 and

*Tb*TRF co-localized in the nucleus (Figure 1C), indicating that *Tb*TIF2 is located at the telomere. Chromatin IP (ChIP) with an HA antibody in these cells showed that telomeric DNA was significantly enriched in the ChIP product (Figure 1D and Supplementary information, Figure S1F), while the 50 bp repeat DNA located upstream of BES promoters was not (Figure 1D and Supplementary information, Figures S1F and S2A). These results indicate that *Tb*TIF2 is a component of *T. brucei* telomere complex.

TbTIF2 is essential for cell viability and mildly affects VSG silencing at some telomeres

To examine the functions of *Tb*TIF2, we established *Tb*TIF2 RNAi strains in a BF strain that express T7 polymerase and Tet repressor and allow inducible expression of the RNAi construct (SM, [50]). One endogenous *Tb*TIF2 allele was also tagged with F2H in these cells. Since these cells express VSG2, we named them 2/TIF2i. Northern blotting using the *Tb*TIF2 probe and western blotting using an HA antibody showed that the levels of *Tb*TIF2 RNA (Supplementary information, Figure S2B) and *Tb*TIF2 protein (Figure 2A) were substantially decreased following induction of *Tb*TIF2 RNAi by doxycycline. *Tb*TIF2-depleted cells experienced a growth arrest within 24 h (Figure 2B), indicating that *Tb*TIF2 is essential for cell proliferation. FACS analysis showed that depletion of *Tb*TIF2 led to a decrease in G1 cells (2C) and an increase in G2/M (4C) and polyploidy cells (6C and 8C) (Supplementary information, Figure S3). This is similar to the situation in mouse cells, where deletion of TIN2 leads to polyploidization resulting from endoreduplication [51].

To explore whether *Tb*TIF2 is involved in regulation of subtelomeric *VSG* expression, we performed quantitative RT-PCR (qRT-PCR) using primers specific to several BES-linked *VSGs*. In 2/TIF2i cells where normally only *VSG2* is active, we observed an ~10-fold derepression of *VSG14* but no significant derepression (consistent, >2-fold increase of mRNA level) of other BES-linked *VSGs* upon depletion of *Tb*TIF2 (Figure 2C). *VSG14* resides in BES8, which is the shortest BES (~10 kb) in our lab strain, containing only *ESAG7*, 70 bp repeats, and *VSG14*, while most other BESs are 40-60 kb long (Supplementary information, Figure S2A) [33]. BES10 is the second shortest BES (25-30 kb) in this strain [33], and we observed occasional, though not consistent derepression of *VSG15* that resides in BES10 (Figure 2C). Thus, *Tb*TIF2 may affect BES promoters that are close to telomeres. Because MESs are monocistronic transcription units whose promoters are usually only 5 kb upstream of the telomere (Supplementary information, Figure S2A),

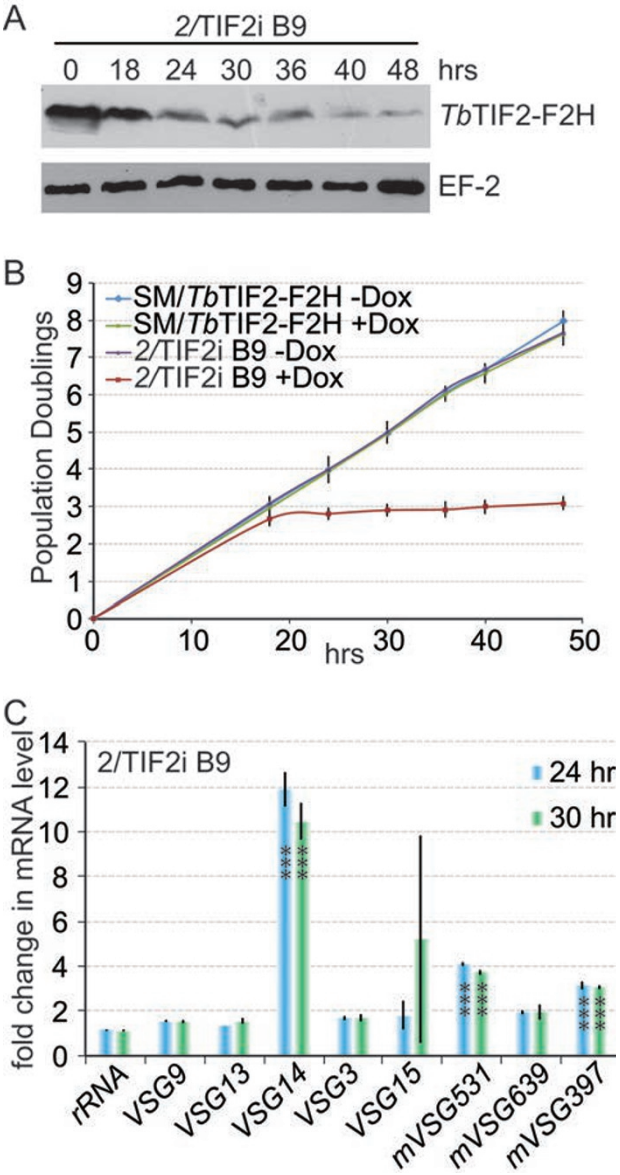

Figure 2 *Tb*TIF2 is essential for cell survival. **(A)** Induction of *Tb*TIF2 RNAi led to a decreased *Tb*TIF2 protein level. Whole cell extracts were prepared from 2/TIF2i clone B9 cells at different time points after induction of *Tb*TIF2 RNAi. HA antibody F-7 and EF-2 antibody (as a loading control, Santa Cruz Biotechnologies) were used in western blotting analyses. **(B)** Depletion of *Tb*TIF2 by RNAi led to a growth arrest in *T. brucei* cells. Growth curves for SM/*Tb*TIF2-F2H and 2/TIF2i cells in the presence (+) or the absence (−) of doxycycline (Dox). Average population doublings were calculated from three independent cultures. **(C)** *Tb*TIF2 depletion had mild effects on subtelomeric *VSG* silencing. mRNA levels for several BES-linked *VSGs* and *mVSGs* were estimated by qRT-PCR at different time points after induction of *Tb*TIF2 RNAi. The fold changes in mRNA levels were calculated from three independent experiments. 0 h values are all equal to "1" but not shown. Changes significantly different from that of rRNA are indicated by asterisks. ***$P < 0.001$ (unpaired *t*-tests).

we tested whether *mVSGs* are affected by *Tb*TIF2 depletion. We examined the mRNA levels of *mVSG531*, *639*, and *397* [52] and found that *mVSG531* and *mVSG397* were derepressed by 3-4-fold upon depletion of *Tb*TIF2 (Figure 2C). In an independent *Tb*TIF2 RNAi strain, S/TIF2i (see below), we observed the same *VSG* derepression pattern: *VSG14* was derepressed by 6-7-fold, while *mVSG539* and *mVSG397* were derepressed by 2-3-fold upon *Tb*TIF2 depletion (Supplementary information, Figure S2C). Therefore, depletion of *Tb*TIF2 led to a mild derepression of certain subtelomeric *VSGs*.

TbTIF2 suppresses VSG switching

To test whether *Tb*TIF2 affects subtelomeric *VSG* switching, we introduced the inducible *Tb*TIF2 RNAi construct into the SM-derived HSTB261 strain, which was designed for *VSG* switching analysis (Supplementary information, Figure S4) [42]. We obtained two independent S/TIF2i clones ("S" stands for "switching"), in which one endogenous *Tb*TIF2 allele was tagged with F2H.

HSTB261 cells carry a *blasticidin resistance* (*BSD*) marker immediately downstream of the active BES promoter and a *puromycin resistance* (*PUR*) gene fused with the *Herpes simplex* virus *thymidine kinase* (*TK*) gene between the 70 bp repeats and the active *VSG2* gene in the same BES (Supplementary information, Figure S4). All *VSG* switchers are expected to lose the expression of *TK* and become resistant to ganciclovir (GCV), a nucleoside analogue, allowing easy selection of *VSG* switchers. Because *Tb*TIF2 is essential for cell survival, we recovered switchers after only transient *Tb*TIF2 depletions. Inducing *Tb*TIF2 RNAi in S/TIF2i cells for 30 h resulted in a transient growth arrest (Figure 3A) and a temporary decrease in *Tb*TIF2 protein level for ~24 h (Figure 3B). The recovered cells experienced a growth arrest again upon reinduction of *Tb*TIF2 RNAi (Supplementary information, Figure S5A), indicating that these cells did not lose the *Tb*TIF2 RNAi construct or the RNAi mechanism.

We performed the switching assay as reported previously [42]. The parental HSTB261 cells, control cells carrying an empty vector (S/v), and two independent S/TIF2i clones (A12 & A14) were incubated with or without doxycycline for 30 h, washed extensively, and allowed to recover for 2-3 days. All cells were cultured for the same number of population doublings to allow a fair comparison of switching frequencies among different strains. Subsequently, cells were plated in the presence of GCV to select for switchers and in the absence of GCV to determine the plating efficiencies. Plating efficiencies (Supplementary information, Figure S5B) were used to normalize the final *VSG* switching frequencies.

We found that a transient depletion of *Tb*TIF2 led to a 4.2-5.8-fold increase in *VSG* switching frequency when compared to S/v cells, while uninduced S/TIF2i and parental cells exhibited similar *VSG* switching frequencies to S/v cells (Figure 3C). To confirm that this effect was specifically due to depletion of *Tb*TIF2, we performed a complementation analysis. An inducible expression vector containing FLAG-HA (FH)-tagged *Tb*TIF2 was transfected into S/TIF2i A14 cells. Culturing S/TIF2i + *Tb*TIF2-FH cells in the presence of doxycycline for 30 h resulted in a decrease in the endogenous *Tb*TIF2 mRNA level (Supplementary information, Figure S5C, left) and a simultaneous increase in *Tb*TIF2-FH mRNA (Supplementary information, Figure S5C, left) and protein (Supplementary information, Figure S5C, right) levels. This induction did not cause cell growth arrest (Supplementary information, Figure S5D). The *VSG* switching frequency in these cells was comparable to that in S/v cells (Figure 3C), indicating that the elevated *VSG* switching frequency was specifically due to depletion of *Tb*TIF2. Therefore, our observations indicate that *Tb*TIF2 suppresses *VSG* switching. The bulk telomeres in S/TIF2i cells are 15 kb long on average, and depletion of *Tb*TIF2 did not result in a dramatic telomere shortening within the time frame of the switching experiment (Supplementary information, Figure S5E). Therefore, increased *VSG* switching following *Tb*TIF2 depletion was not due to extremely short telomeres.

VSG switching can occur through several pathways including *in situ* switching, crossover (CO), *VSG* and ES gene conversion (GC), and ES loss + *in situ* switching. By examining marker genotypes and antibiotic resistance phenotypes in the recovered switchers, we can determine the mechanism of a given switching event (Supplementary information, Figure S4). However, this assay cannot differentiate between ES GC and ES loss + *in situ* events. These can only be differentiated by pulsed-field gel electrophoresis (PFGE) of intact chromosomes followed by Southern analysis. The majority of switchers in *Tb*TIF2-depleted and control cells (~90%) arose from *VSG* GC and ES GC/ES loss + *in situ* events (Figure 3D), suggesting that GC is the predominant mechanism of *VSG* switching under these conditions. ES GC/ES loss + *in situ* is most popular (60%-75%) in control cells and became even more prevalent when *Tb*TIF2 was transiently depleted (> 80%; Figure 3D), indicating that there were more subtelomeric gene rearrangements when *Tb*TIF2 was depleted. Therefore, *Tb*TIF2 is important for subtelomere stability. To verify each *VSG* switching mechanism in several representative switchers, we determined their active *VSGs* by RT-PCR using a spliced leader primer (common to all *T. brucei* mRNAs) and

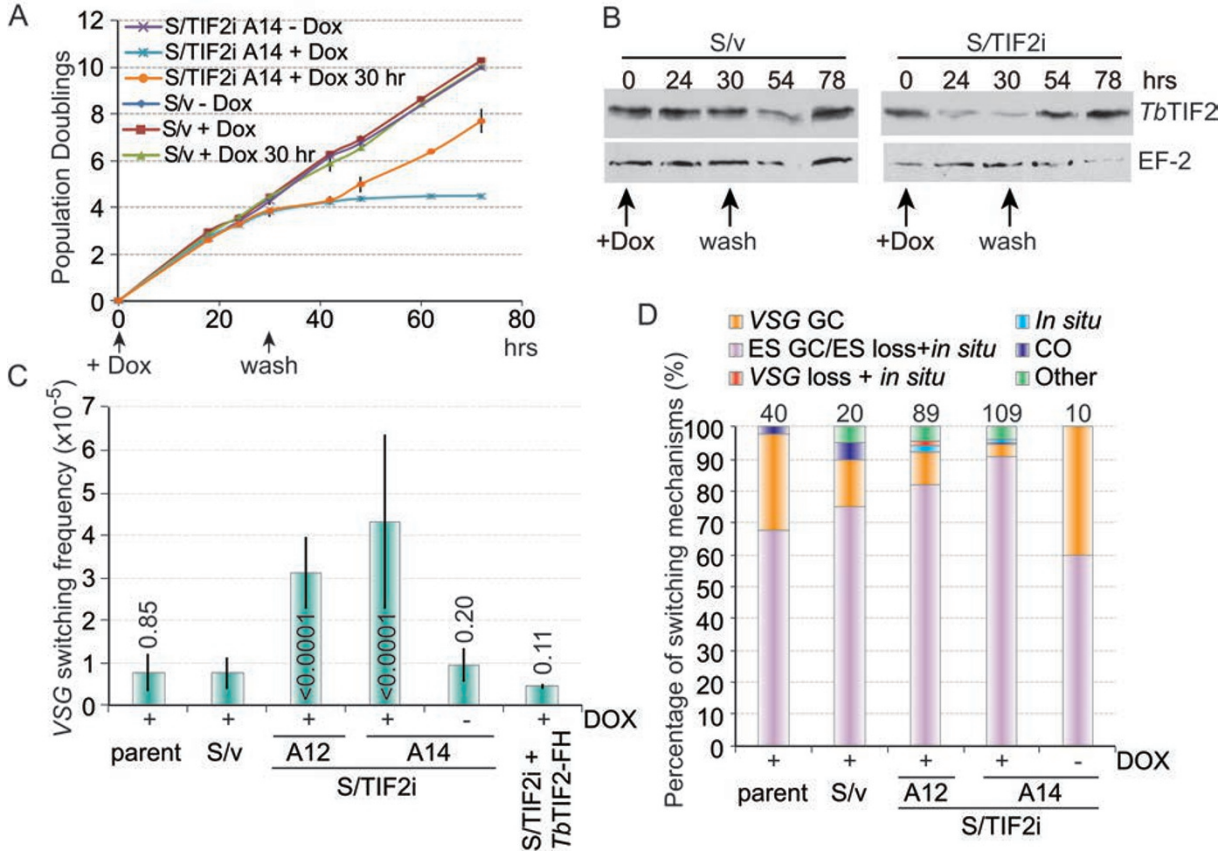

Figure 3 Transient depletion of *Tb*TIF2 led to an elevated *VSG* switching frequency. **(A)** Induction of *Tb*TIF2 for 30 h led to a growth arrest for ~24 h. S/TIF2i clone A14 and S/v cells were cultured without doxycycline, with doxycycline for 30 h, or with doxycycline throughout the experiment. Average population doublings were calculated from four independent experiments to plot the growth curve. **(B)** The *Tb*TIF2 protein level decreased for ~24 h when *Tb*TIF2 RNAi was induced for 30 h in S/TIF2i cells. Western blotting analyses were performed using HA antibody F-7 and EF-2 antibody. S/v cells were treated the same way as a control. **(C)** *VSG* switching frequencies in S/TIF2i and control cells. Cells were cultured with doxycycline for 30 h or without doxycycline as indicated. Average switching frequencies were calculated from 4-12 independent assays. *P*-values (unpaired *t*-tests) between S/v and other cells are shown as numbers on top of the corresponding columns. **(D)** *VSG* switching pathways in S/TIF2i and control cells. Percent of each *VSG* switching pathway of total events was plotted. Listed on top of each column is the number of switchers analyzed. Detailed switcher characterization results are listed in Supplementary information, Tables S3-S6.

a *VSG* C-terminal primer (common to *VSGs*) followed by sequencing analysis. PFGE of intact chromosomes from these switchers followed by Southern analyses using probes specific for *VSG2*, *BSD*, and the newly active *VSG* confirmed all predicted switching mechanisms (Supplementary information, Figure S6). ES loss + *in situ* switchers were present in both the parental strain and *Tb*TIF2-depleted cells (Supplementary information, Figure S6; data not shown), indicating that this mechanism is not unique in *Tb*TIF2 RNAi cells.

Depletion of TbTIF2 increased DSBs in subtelomeric BESs

Because most *VSG* switchers arose from HR-mediated events, we wondered whether depletion of *Tb*TIF2 led to more DSBs in subtelomeric BESs. We performed a Ligation-Mediated PCR (LMPCR) assay to directly detect DSBs along BESs [10, 43]. In this assay, a double-stranded adaptor with a blunt end and a staggered end was ligated to genomic DNA at the DSB followed by PCR using locus-specific primers and Southern analysis (Figure 4A). Blunt-ended broken DNA can be ligated to the blunt end of the adaptor directly, while staggered broken DNA ends can be converted to blunt ends by T4 DNA polymerase before ligation. The staggered end of the adaptor and single-stranded DNA breaks are not expected to be ligated in this assay [53].

Following induction of *Tb*TIF2 RNAi for 24 h, we

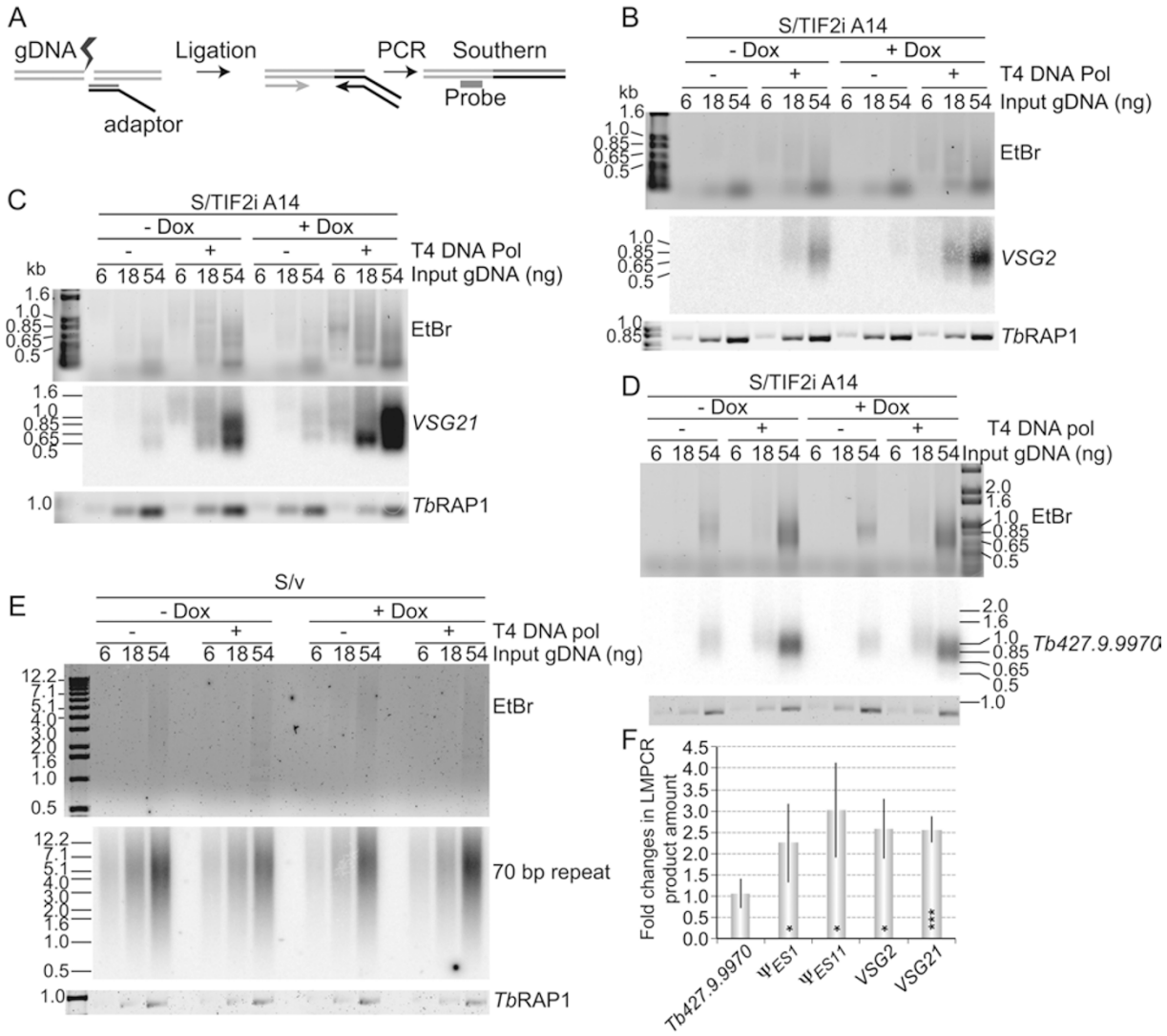

Figure 4 Depletion of *Tb*TIF2 led to increased amount of DSBs at subtelomeric BES regions. **(A)** The principle of LMPCR. LMPCR analyses were performed in S/TIF2i clone A14 **(B-D)** and S/v **(E)** cells. The LMPCR products were hybridized with *VSG2* **(B)**, *VSG21* **(C)**, *Tb427.9.9970* (which encodes a putative small nuclear RNA gene activation protein 50, SNAP50) **(D)**, and 70 bp repeat **(E)** probes. In each panel of this figure and Figure 6, the Ethidium bromide (EtBr)-stained LMPCR products are shown at the top, the Southern blot result is shown in the middle, and the PCR products using primers specific to *Tb*RAP1 are shown at the bottom as a loading control. The amounts of input genomic DNA, either treated (+) or untreated (−) with T4 DNA polymerase, were marked on top of each lane. Molecular weight markers (in kb unless otherwise indicated) are labeled on the left. **(F)** The signal intensities of LMPCR products (treated with T4 DNA polymerase) were quantified by ImageQuant from Southern blots exposed to phosphorimagers. The fold changes were calculated by dividing post *Tb*TIF2 depletion value by preinduction value. The average was calculated from at least three independent experiments. Error bars represent standard deviation. *P*-values (unaired *t*-tests) were calculated using Graphpad Prism between values at each subtelomeric locus and that at *Tb427.9.9970*. Asterisks indicate significant difference. **P* < 0.05; ***P* < 0.01; ****P* < 0.001.

detected substantially more LMPCR products at BES promoter (Supplementary information, Figure S7A) and 70 bp repeat regions (Supplementary information, Figure S7B), indicating that *Tb*TIF2 is important for subtelomere integrity. Since all BESs have nearly identical promoter and 70 bp repeat sequences [33], these results did not distingusih whether DSBs are in the active or silent BESs. We therefore used specific probes to detect DSBs at active or silent single-copy gene loci. Because LMPCR is semiquantitative, it is unfair to compare the absolute amount of DSBs at different loci due to possible different PCR amplification efficiencies and

different probe hybridization efficiencies. We therefore estimated the change of DSB amount before and after depletion of *Tb*TIF2 at individual locus, then compared whether *Tb*TIF2 has similar effects at different loci. To avoid variation that resulted from different RNAi inductions, we performed LMPCR at two pairs of active and silent loci using genomic DNA isolated from the same induction experiments. We observed increased amount of LMPCR products following *Tb*TIF2 depletion at the active *VSG2* (Figure 4B) and the silent *VSG21* (Figure 4C) loci. Ψ_{BES1} and Ψ_{BES11} are unique *VSG* pseudogenes in the active *VSG2*-containing BES1 and the silent *VSG16*-containing BES11, respectively (Supplementary information, Figure S7I, top) [33, 45]. We observed increased LMPCR products at Ψ_{BES1} (Supplementary information, Figure S7C) and Ψ_{BES11} (Supplementary information, Figure S7D) loci, too. Quantification of LMPCR signals (in ImageQuant) from at least three sets of independent experiments showed similar fold of increase at all four loci (Figure 4F), indicating that *Tb*TIF2 depletion led to similar increases in DSB levels in both active and silent BESs.

Subsequently, we performed the LMPCR analysis in an independent *Tb*TIF2 RNAi strain (9/TIF2i) that expresses VSG9 and carries *BSD* at the active BES promoter and *PUR* at the silent *VSG2*-containing BES promoter (Supplementary information, Figure S7I, bottom) [45]. Again, we detected more LMPCR products at both loci after depletion of *Tb*TIF2 (Supplementary information, Figure S7E and S7F), indicating that this phenotype was not specific for any particular VSG expresser. In contrast, approximately the same levels of LMPCR products were detected at a random single-copy chromosomal locus (*Tb*427.9.9970) before and after *Tb*TIF2 depletion (Figure 4D and 4F), suggesting that *Tb*TIF2 influences DSB amount primarily at subtelomeric regions. In most cases, blunt-ended DSBs represented a small fraction of all breaks (Figure 4 and Supplementary information, Figure S7, compare + and −T4 DNA polymerase). *Tb*TIF2 depletion induced both blunt and stagger ended DSBs. As a control, S/v cells were examined the same way and we did not detect elevated LMPCR products at 70 bp repeats (Figure 4E), the Ψ_{BES1} locus (Supplementary information, Figure S7G), or BES promoters (Supplementary information, Figure S7H). The increased DSB amount in *Tb*TIF2 depleted cells could result from increased DSB formation or decreased DSB repair. Our current assay cannot differentiate between these two possibilities. Nevertheless, our data demonstrate that *Tb*TIF2 plays an important role in subtelomere integrity maintenance.

We also examined whether depletion of *Tb*TIF2 altered chromatin structure by the Formaldehyde-Assisted Isolation of Regulatory Elements (FAIRE) analysis [54]. In this assay, chromatin is fixed by formaldehyde. After sonication, nucleosome-free DNA fragments are enriched in the phenol-chloroform extracted fraction. We compared the FAIRE-extracted DNA before and after *Tb*TIF2 depletion at several subtelomeric *VSG* loci, BES promoters, and a random chromosomal locus (*Tb*427.2.2440) in S/TIF2i, 2/TIF2i, and S/v cells. We only observed a mild change in FAIRE-extracted DNA before and after depletion of *Tb*TIF2 at some *VSG* loci (Supplementary information, Figure S5F). Thus, *Tb*TIF2 depletion does not affect chromatin structure significantly, suggesting that such changes are unlikely the main reason for elevated *VSG* switching frequency.

Depletion of TbTIF2 significantly increases association of TbRAD51 with the active BES

*Tb*RAD51 and some of its paralogues are required for most *VSG* switching events [38, 39]. Since *Tb*TIF2 depletion elevated the DSB amount at BESs, we hypothesized that more *Tb*RAD51 might associate with BESs. To test this, we first performed immunofluorescence using the *Tb*RAD51 antibody. *Tb*RAD51 forms distinct foci in cell nuclei in response to DNA damage [55]. Indeed, in WT SM/*Tb*TIF2-F2H cells treated with phleomycin, we observed large, bright *Tb*RAD51 foci in the nucleus (Supplementary information, Figure S8A, right). In 2/TIF2i cells treated with doxycycline, we observed similar distinct *Tb*RAD51 foci in the nucleus (Supplementary information, Figure S8B, right), confirming that depletion of *Tb*TIF2 led to an elevated amount of DSBs. In contrast, in untreated 2/TIF2i cells (Supplementary information, Figure S8B, left) or in WT cells treated with or without doxycycline (Supplementary information, Figure S8A, middle and left), *Tb*RAD51 did not form distinct large foci in the nucleus but gave a hazy staining pattern. A significant increase in the number of cells that have distinct *Tb*RAD51 foci was seen when *Tb*TIF2 was depleted (Figure 5A). Therefore, depletion of *Tb*TIF2 resulted in a DNA damage response-like phenotype where *Tb*RAD51 forms distinct foci in the nucleus.

To further determine whether *Tb*RAD51 exhibited an increased association with telomeres and subtelomeres in *Tb*TIF2-depleted cells, we performed ChIP analysis using the *Tb*RAD51 antibody in S/TIF2i cells. Depletion of *Tb*TIF2 led to an increase in the association of *Tb*RAD51 with TTAGGG and 50 bp repeats, suggesting that *Tb*TIF2 dysfunction led to more DSBs at telomeres and subtelomeres (Figure 5B). Our *T. brucei* strain has nearly 250 telomeres due to its ~100 minichromosomes in addition to 11 pairs of megabase chromosomes and a few intermediate chromosomes. However, there are only

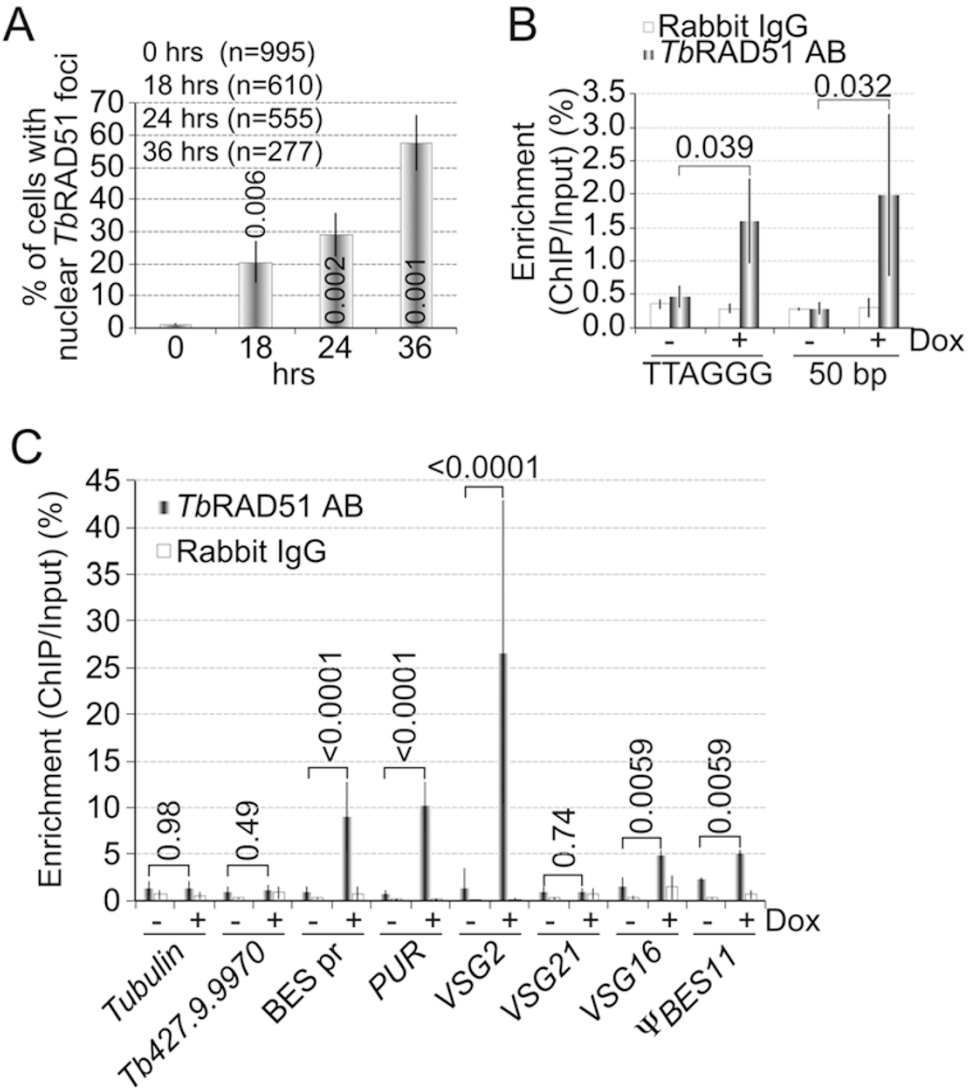

Figure 5 Depletion of *Tb*TIF2 led to increased *Tb*RAD51 association with telomeric and subtelomeric chromatin. **(A)** Quantification of cells with punctate nuclear *Tb*RAD51 foci at various time points after induction of *Tb*TIF2 RNAi in S/TIF2i A14 cells. Number of cells counted was indicated in the parentheses. Averages were calculated from three independent experiments. Numbers on columns indicate *P*-values (unpaired *t*-tests) compared to the 0 h value. **(B**, **C)** ChIP analysis using the *Tb*RAD51 antibody or rabbit IgG. ChIP products and input DNA were hybridized with either a TTAGGG or a 50 bp repeat probe in Southern blotting, which were exposed to a phosphorimager. The hybridization signal intensity was quantified by ImageQuant, and averages were calculated from four independent experiments **(B)**. ChIP products were analyzed by qPCR using primer pairs specific to various loci (Supplementary information, Table S1). Averages were calculated from 5-10 independent experiments **(C)**. In both **B** and **C**, numbers on top of brackets indicate *P*-values (unpaired *t*-tests) comparing *Tb*RAD51 ChIP values before and after *Tb*TIF2 depletion.

nearly 20 BESs. The level of increase in *Tb*RAD51 association with TTAGGG and 50 bp repeats is similar (Figure 5B), suggesting that *Tb*RAD51 might be recruited to individual BESs at higher concentration than to individual telomeres that do not have any adjacent BES. To achieve better resolution, we performed ChIP experiments using the *Tb*RAD51 antibody followed by qPCR using primers specific to BES promoters, *PUR* and *VSG2* in the active BES, and *VSG21, VSG16,* and Ψ_{BES11} in silent BESs (Supplementary information, Figure S7I, top) [45]. We observed a significant increase in the association of *Tb*RAD51 with BES promoters, *PUR*, and *VSG2* (Figure 5C), confirming that *Tb*RAD51 associated more with subtelomeric BESs upon *Tb*TIF2 depletion. Surprisingly,

this increase was mostly restricted in the active BES, since the association of *Tb*RAD51 with the silent *VSG21* was not significantly changed (Figure 5C). Although more *Tb*RAD51 associated with the silent *VSG16* and Ψ_{BES11}, the increase was not as dramatic as that at the active *VSG2* locus (Figure 5C). Since we observed similar increases in DSB amounts at both active and silent BESs upon depletion of *Tb*TIF2 (Figure 4F), this observation suggests that *Tb*RAD51 preferentially associates with DSBs in the active BES. No significant increase was observed for the association of *Tb*RAD51 with the chromosome internal tubulin array or the *Tb*427.9.9970 locus (Figure 5C), supporting our conclusion that depletion of *Tb*TIF2 does not induce DSBs at chromosome internal loci.

Subtelomeric DSBs in TbTIF2-depleted cells are further increased by TbRAD51 disruption

Upon depletion of *Tb*TIF2, DSB levels increased at subtelomeric BESs, as did association of *Tb*RAD51 with the active BES, indicating that *Tb*RAD51 associates with and repairs DSBs in the active BES, which can lead to *VSG* switching, while DSBs in silent BESs may not be repaired by *Tb*RAD51-mediated HR. To test this hypothesis, we deleted both alleles of *Tb*RAD51 in S/TIF2i cells and tried to perform the *VSG* switching assay. However, these cells were less healthy than the S/TIF2i cells, and even a transient induction of *Tb*TIF2 RNAi resulted in an irreversible cell growth arrest, preventing us from carrying out switching assays.

We therefore performed LMPCR in the S/TIF2i/*Tb*RAD51Δ cells. Similar to S/TIF2i cells, depletion of *Tb*TIF2 increased DSB levels at BES promoters (Supplementary information, Figure S9A), 70 bp repeats (Supplementary information, Figure S9B), active Ψ_{BES1} (Figure 6A), silent Ψ_{BES11} (Figure 6B), active *VSG2* (Supplementary information, Figure S9C), and silent *VSG21* (Supplementary information, Figure S9D) loci. More strikingly, the amount of DSBs at subtelomeric BESs were much higher when *Tb*RAD51 was deleted than when it was not (Figure 6 and Supplementary information, S9), indicating that loss of *Tb*RAD51 exacerbated the increased DSB phenotype in *Tb*TIF2-depleted cells. To avoid variations between different inductions and LMPCR experiments, we always induced S/TIF2i and S/TIF2i/*Tb*RAD51Δ cells at the same time using exactly the same conditions. By quantifying the signal intensity of LMPCR products, we found that after depletion of *Tb*TIF2, the amount of DSBs in the *Tb*RAD51Δ background was 2.7-fold and 4.5-fold of that in the *Tb*RAD51 wild-type background at the active *VSG2* and Ψ_{BES1} locus, respectively, but only 1.6-fold and 1.5-fold at the silent *VSG21* and Ψ_{BES11} locus, respectively (Figure 6C). This suggests that DSBs in the active BES were preferentially repaired by *Tb*RAD51-dependent mechanism.

Discussion

Telomere proteins and antigenic variation

Our current and previous studies showed that *T. brucei* telomere proteins play important roles in antigenic variation, monoallelic *VSG* expression and *VSG* switching, which are critical pathogenesis mechanisms in *T. brucei* [45, 46]. Among the three known *T. brucei* telomere proteins, *Tb*TIF2 suppresses *VSG* switching but only mildly affects BES promoters that are close to telomeres. This is different from *Tb*RAP1, depletion of which led to dramatic subtelomeric *VSG* derepression [45, 46]. In contrast, *Tb*TIF2's effect on *VSG* silencing is similar to that of *Tb*TRF, which does not affect BES-linked *VSG* silencing [45]. Although both *Tb*TIF2 and *Tb*RAP1 interact with *Tb*TRF, the interaction between *Tb*TIF2 and *Tb*TRF is much stronger than that between *Tb*RAP1 and *Tb*TRF based on yeast two-hybrid and co-IP analyses (this study and [45]). Our observations suggest that *Tb*TIF2 may function in the same pathway as *Tb*TRF but not *Tb*RAP1. Further studies of functions of *Tb*TRF and *Tb*RAP1 in *VSG* switching would shed more light on the interplay between *T. brucei* telomere proteins in antigenic variation.

Telomere proteins in subtelomere integrity and stability maintenance

In this study, we found that depletion of *Tb*TIF2 increased DSBs at subtelomeres and elevated recombination events that lead to *VSG* switching, demonstrating that *Tb*TIF2, a telomere protein, is important for maintaining subtelomere integrity and stability.

More *Tb*RAD51 associates with telomeric DNA upon *Tb*TIF2 depletion, indicating that *Tb*TIF2 depletion led to more telomeric DSBs. This is consistent with the notion that telomere proteins are important for protecting chromosome ends [11]. Loss of mammalian TIN2 led to both chromatid-type and chromosome-type telomere fusions [51]. It is possible that *Tb*TIF2 depletion results in similar telomere fusions and subsequent breakage-fusion-bridge cycle, which can result in DNA amplification and large terminal deletions [57]. Some of the ES loss + *in situ* switching that we observed might have been a consequence of the breakage-fusion-bridge cycle, although telomere fusions have not been reported in *T. brucei*. It was reported previously that a considerable percent (22%) of cells with DSBs downstream of the active *VSG* lose the whole active BES [10]. *Tb*TIF2 depletion-induced

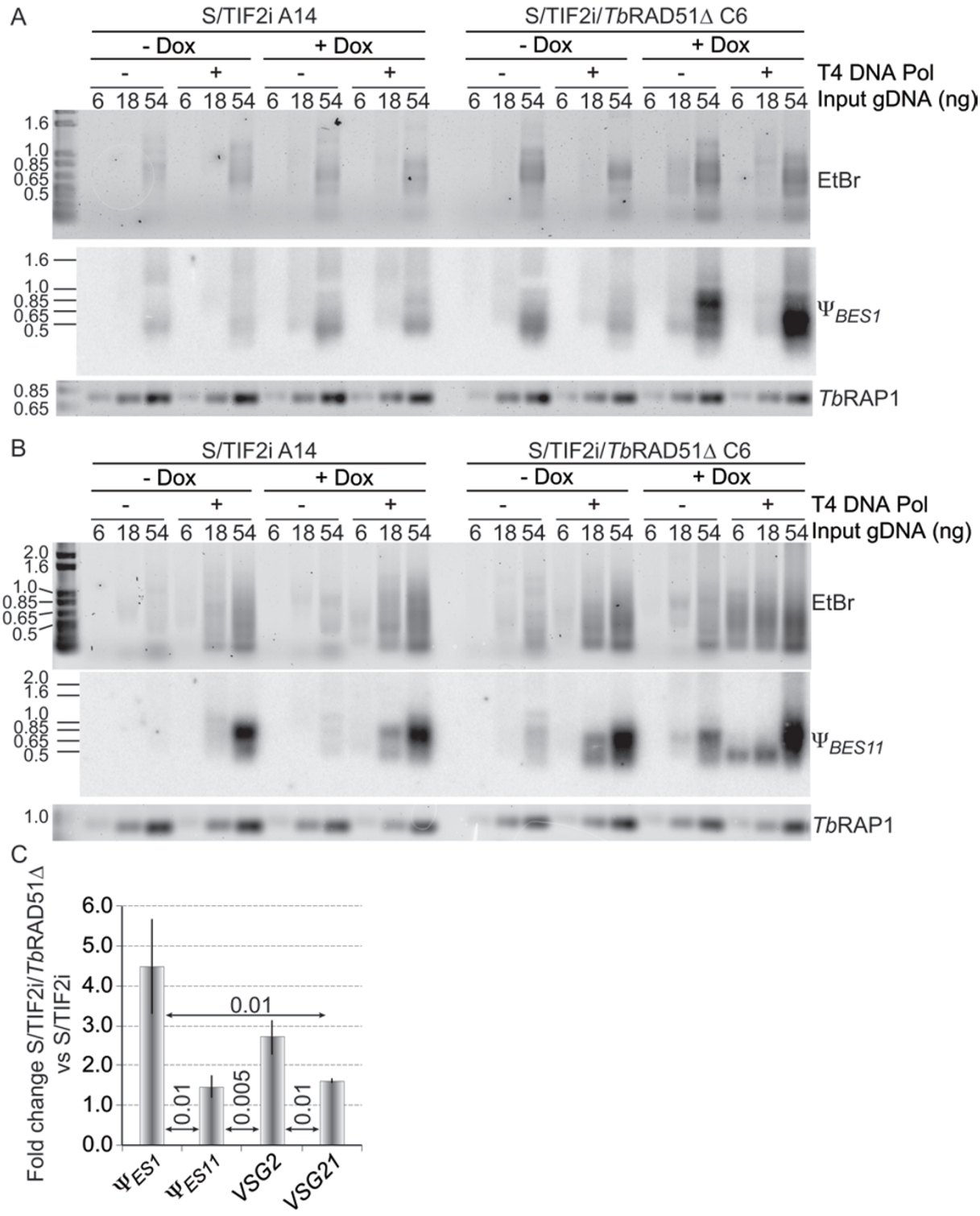

Figure 6 More subtelomeric DSBs persisted when *Tb*RAD51 was deleted in *Tb*TIF2-depleted cells. The LMPCR products from S/TIF2i A14 and S/TIF2i/*Tb*RAD51Δ C6 cells were hybridized with the Ψ_{BES1} **(A)** or Ψ_{BES11} **(B)** probe. **(C)** The signal intensities of LMPCR products (treated with T4 DNA polymerase) were quantified by ImageQuant from Southern blots exposed to phosphorimagers. The fold changes were calculated by dividing post *Tb*TIF2 depletion value in S/TIF2i/Δ*Tb*RAD51 cells by that in S/TIF2i cells on the same gel. The average was calculated from at least three independent experiments. Error bars represent standard deviation. *P*-values (unpaired *t*-tests) between pairs of loci were indicated.

DSBs were detected at subtelomeres including the region downstream of the active *VSG2*, which may also explain why we obtained ES loss + *in situ* switchers.

*Tb*TIF2 may contribute to subtelomere stability through other means. First, *Tb*TIF2 may be required for proper telomeric DNA replication, as some telomere proteins do in other organisms [23, 24, 26]. Fork stalling in the absence of *Tb*TIF2 could increase DSB formation at the telomere vicinity, and increased DNA topological stress could also lead to more DSBs at subtelomeres. Second, *Tb*TIF2 may play an important role in telomere cohesion formation/maintenance. Mammalian TIN2 interacts with SA1 [27, 28], an ortholog of SCC3 and a telomere-specific cohesin subunit that is important for sister telomere cohesion. *Tb*TIF2 is a functional homolog of TIN2 and may have similar functions to TIN2. Defective sister telomere pairing due to *Tb*TIF2 depletion could lead to low efficiency of DNA damage repair via the sister chromatid, resulting in more DSBs in subtelomeric BESs. This in turn could lead to loss of terminal chromosome fragments. In addition, a lack of sister telomere pairing is expected to allow more flexible pairing and HR between non-sister telomeres, which in turn may result in more frequent *VSG* switching. The predominant *VSG* switching pathway is ES GC/ES loss + *in situ* switching in *Tb*TIF2-depleted cells, which is consistent with this hypothesis. Interestingly, partial depletion of *Tb*SCC1 or other cohesin subunits *Tb*SMC1 and *Tb*SCC3 also led to premature dissociation of sister chromatids at the active BES and increased *VSG* switching frequency [58], although *in situ* switching appears to be the preferred pathway in cohesion-defective cells, which is not exactly the same as in *Tb*TIF2-depleted cells, where a significant portion of the *VSG* switchers arose from ES loss + *in situ* or ES GC switching. Our first model that *Tb*TIF2 is important for telomeric DNA replication suggests that more DSB formation is the reason for more subtelomeric DSBs in *Tb*TIF2-depleted cells, while the second model suggests that less DSB repair is the reason. However, both factors could contribute to the observed phenotypes. More investigations are necessary to further discern these two underlying mechanisms.

TbRAD51-dependent HR-mediated DNA damage repair and VSG switching

RAD51 is a major player in HR-mediated DNA damage repair [37]. *VSG* switching is mostly dependent on *Tb*RAD51 [39], its paralogue *Tb*RAD51-3 [38], and its interacting factor BRCA2 [40]. In addition, HR-mediated GC events are the preferred mechanism for *VSG* switching in our lab strain [39, 42]. Depletion of *Tb*TIF2 led to more DSBs at subtelomeric BESs and an increased *Tb*RAD51 association with subtelomeric chromatin. *Tb*RAD51 disruption further increased subtelomeric DSBs in *Tb*TIF2-depleted cells. These observations indicate that *Tb*RAD51-mediated HR is a major pathway for repair of the elevated DSBs at subtelomeres. Repair of these induced DSBs presumably contributed to the increased *VSG* switching frequency in *Tb*TIF2-depleted cells. In S/TIF2i/*Tb*RAD51Δ cells, the DSBs induced by *Tb*TIF2 depletion were not repaired due to the lack of *Tb*RAD51, which is likely the reason for subsequent cell lethality.

*Tb*TIF2 depletion led to increased *Tb*RAD51 association with subtelomeric chromatin, which was more at active loci than at silent loci. In addition, we detected stronger increases of DSBs at the active loci than at the silent loci in S/TIF2i/*Tb*RAD51Δ cells. The extra DSBs detected in the *Tb*RAD51Δ background were presumably repaired by *Tb*RAD51 in S/TIF2i cells. *Tb*TIF2 depletion induced similar level of DSBs at the active and silent loci. Therefore, *Tb*RAD51 preferentially repairs DSBs in the active BES. The active BES differs from silent BESs in that it is actively transcribed by RNA polymerase I [59]. In addition, the active BES forms an open chromatin structure depleted of most nucleosomes, while silent BESs are packed with nucleosomes [60, 61]. Our data suggest that the transcriptional status and/or the chromatin structure of the DSB site may influence the choice of DSB repair mechanism. In yeast, two independent HR pathways are involved in telomere maintenance in telomerase-negative cells [62]: amplification of subtelomeric Y′ elements is RAD51-dependent, while amplification of telomeric repeats is RAD50-dependent. In *T. brucei,* DSBs at silent BESs can be repaired by *Tb*RAD51-independent microhomology-mediated end joining [10] or possibly other mechanisms such as *Tb*RAD50-dependent pathway. However, more studies are necessary to test this hypothesis. A RAD50 DNA repair-like protein (*Tb*427tmp.01.0340) has been annotated in TriTrypDB, although its characterization has not been reported. Alternatively, DSBs in silent BESs are well tolerated and may not be repaired, as loss of BES following DSB induction in silent BESs has been observed frequently [10].

Telomere protein evolution from protozoa to mammals

We have identified *Tb*TIF2 as a functional homolog of TIN2. *Tb*TIF2 does not have any telomere DNA binding domains, thus it relies on *Tb*TRF to localize to the telomere, which is presumably essential for its function in subtelomere integrity and stability maintenance. It is worth noting that human TRF2 interacts with Apollo in the same way that human TRF1 interacts with TIN2. Apollo and TIN2 share a conserved TRF-interacting mo-

tif Y/F-X-L-X-P, where X can be any residue [49]. Interestingly, *Tb*TIF2 has a Y-F-L-C-P motif at its C-terminus (Supplementary information, Figure S1D). However, yeast two-hybrid analysis showed that the C-terminal half of *Tb*TIF2 did not interact with *Tb*TRF. A careful examination of the *Tb*TRF sequence showed that *Tb*TRF lacks the conserved region in the TRFH domain of human TRF1 and TRF2 that is essential for recognizing the Y/F-X-L-X-P motif [48], explaining why the C-terminus of *Tb*TIF2 does not interact with *Tb*TRF. Therefore, although the TIN2-TRF/*Tb*TIF2-*Tb*TRF interaction is conserved, the detailed interaction surfaces on the two protein pairs have changed through evolution. This makes the interaction domain between *Tb*TRF and *Tb*TIF2 an attractive target for anti-parasite agents, as the interaction is specific for *T. brucei* and not present in its host.

Materials and Methods

ChIP

ChIP was performed according to [64]. ChIP products were hybridized with a TTAGGG or a 50-bp repeat probes in slot blot analysis. Alternatively, qPCR using primers specific to various BES loci (Supplementary information, Table S1) was performed to detect unique sequences in ChIP products.

LMPCR

LMPCR were performed according to [43]. More details are described in Supplementary information, Data S1. Primers used in LMPCR are listed in Supplementary information, Table S2.

VSG switching assay

Switching assays were performed according to [42]. Additional details are described in Supplementary information, Data S1. Detailed switcher analyses are listed in Supplementary information, Tables S3-S6.

FAIRE

FAIRE was performed according to [46] except that the amount of isolated DNA was estimated by qPCR using SsoAdvanced SYBR Green in a CFX96 Connect (Bio-Rad). The FAIRE result was calculated by dividing FAIRE-extracted DNA amount with the input DNA amount, and the fold changes in FAIRE results between *Tb*TIF2-depleted and uninduced cells were plotted.

qRT-PCR

qRT-PCR was performed as described previously [45] except that the samples were analyzed using SsoAdvanced SYBR Green in a CFX96 Connect (Bio-Rad). Primers used in qRT-PCR are described in the previous study [45].

Yeast two-hybrid analyses

Yeast two-hybrid analyses were carried out as described in [48].

Immunofluorescence

Immunofluorescence was carried out as described in [48]. Cell images were captured by a DeltaVision image restoration microscope (Applied Precision/Olympus), deconvoluted by using measured point spread functions, and edited with Photoshop.

Acknowledgments

We thank Dr Hee-Sook Kim and Dr George AM Cross for sending us the HSTB261 cells, the *Tb*RAD51 knockout and Cre expression constructs, and VSG antibodies. We are very grateful to Dr Richard McCulloch for providing us with the *Tb*RAD51 antibody, and Dr Keith Gull for providing tubulin antibodies. We thank The Rockefeller University proteomics resource center and particularly Dr Joseph Fernandez for carrying out the mass spectrometry analysis. We thank Dr Valentin Börner, Dr Aaron Severson, and Li lab members for their comments on the manuscript. We also thank Vishal Nanavaty for technical support. This work is in part supported by an NIH grant (AI066095), the CSU 2010 Faculty Research and Development award to B Li, and Center for Gene Regulation in Health and Disease at CSU.

References

1 Gabriels J, Beckers MC, Ding H, *et al*. Nucleotide sequence of the partially deleted D4Z4 locus in a patient with FSHD identifies a putative gene within each 3.3 kb element. *Gene* 1999; **236**:25-32.
2 van der Maarel SM, Frants RR, Padberg GW. Facioscapulohumeral muscular dystrophy. *Biochim Biophys Acta* 2007; **1772**:186-194.
3 DeScipio C. The 6p subtelomere deletion syndrome. *Am J Med Genet C Semin Med Genet* 2007; **145C**:377-382.
4 Stewart DR, Kleefstra T. The chromosome 9q subtelomere deletion syndrome. *Am J Med Genet C Semin Med Genet* 2007; **145C**:383-392.
5 Trask BJ, Friedman C, Martin-Gallardo A, *et al*. Members of the olfactory receptor gene family are contained in large blocks of DNA duplicated polymorphically near the ends of human chromosomes. *Hum Mol Genet* 1998; **7**:13-26.
6 Li B. Telomere components as potential therapeutic targets for treating microbial pathogen infections. *Front Oncol* 2012; **2**:156.
7 Mefford HC, Trask BJ. The complex structure and dynamic evolution of human subtelomeres. *Nat Rev Genet* 2002; **3**:91-102.
8 Linardopoulou EV, Williams EM, Fan Y, Friedman C, Young JM, Trask BJ. Human subtelomeres are hot spots of interchromosomal recombination and segmental duplication. *Nature* 2005; **437**:94-100.
9 Teytelman L, Eisen MB, Rine J. Silent but not static: accelerated base-pair substitution in silenced chromatin of budding yeasts. *PLoS Genet* 2008; **4**:e1000247.
10 Glover L, Alsford S, Horn D. DNA break site at fragile subtelomeres determines probability and mechanism of antigenic variation in African trypanosomes. *PLoS Pathog* 2013; **9**:e1003260.
11 Stewart JA, Chaiken MF, Wang F, Price CM. Maintaining the end: roles of telomere proteins in end-protection, telomere replication and length regulation. *Mutat Res* 2012; **730**:12-19.
12 de Lange T. Shelterin: the protein complex that shapes and safeguards human telomeres. *Genes Dev* 2005; **19**:2100-2110.

13 Chong L, van Steensel B, Broccoli D, *et al*. A human telomeric protein. *Science* 1995; **270**:1663-1667.
14 Broccoli D, Smogorzewska A, Chong L, de Lange T. Human telomeres contain two distinct Myb-related proteins, TRF1 and TRF2. *Nat Genet* 1997; **17**:231-235.
15 Bilaud T, Brun C, Ancelin K, Koering CE, Laroche T, Gilson E. Telomeric localization of TRF2, a novel human telobox protein. *Nat Genet* 1997; **17**:236-239.
16 Xin H, Liu D, Wan M, *et al*. TPP1 is a homologue of ciliate TEBP-beta and interacts with POT1 to recruit telomerase. *Nature* 2007; **445**:559-562.
17 Kim SH, Kaminker P, Campisi J. TIN2, a new regulator of telomere length in human cells. *Nat Genet* 1999; **23**:405-412.
18 Houghtaling BR, Cuttonaro L, Chang W, Smith S. A dynamic molecular link between the telomere length regulator trf1 and the chromosome end protector TRF2. *Curr Biol* 2004; **14**:1621-1631.
19 Ye JZ, Hockemeyer D, Krutchinsky AN, *et al*. POT1-interacting protein PIP1: a telomere length regulator that recruits POT1 to the TIN2/TRF1 complex. *Genes Dev* 2004; **18**:1649-1654.
20 Ye JZ, Donigian JR, van Overbeek M, *et al*. TIN2 binds TRF1 and TRF2 simultaneously and stabilizes the TRF2 complex on telomeres. *J Biol Chem* 2004; **279**:47264-47271.
21 Kim SH, Beausejour C, Davalos AR, Kaminker P, Heo SJ, Campisi J. TIN2 mediates functions of TRF2 at human telomeres. *J Biol Chem* 2004; **279**:43799-43804.
22 Denchi EL, de Lange T. Protection of telomeres through independent control of ATM and ATR by TRF2 and POT1. *Nature* 2007; **448**:1068-1071.
23 Sfeir A, Kosiyatrakul ST, Hockemeyer D, *et al*. Mammalian telomeres resemble fragile sites and require TRF1 for efficient replication. *Cell* 2009; **138**:90-103.
24 Ye J, Lenain C, Bauwens S, *et al*. TRF2 and apollo cooperate with topoisomerase 2alpha to protect human telomeres from replicative damage. *Cell* 2010; **142**:230-242.
25 Muraki K, Nabetani A, Nishiyama A, Ishikawa F. Essential roles of Xenopus TRF2 in telomere end protection and replication. *Genes Cells* 2011; **16**:728-739.
26 Miller KM, Rog O, Cooper JP. Semi-conservative DNA replication through telomeres requires Taz1. *Nature* 2006; **440**:824-828.
27 Canudas S, Houghtaling BR, Kim JY, Dynek JN, Chang WG, Smith S. Protein requirements for sister telomere association in human cells. *EMBO J* 2007; **26**:4867-4878.
28 Canudas S, Smith S. Differential regulation of telomere and centromere cohesion by the Scc3 homologues SA1 and SA2, respectively, in human cells. *J Cell Biol* 2009; **187**:165-173.
29 Canudas S, Houghtaling BR, Bhanot M, *et al*. A role for heterochromatin protein 1gamma at human telomeres. *Genes Dev* 2011; **25**:1807-1819.
30 Barry JD, McCulloch R. Antigenic variation in trypanosomes: enhanced phenotypic variation in a eukaryotic parasite. *Adv Parasitol* 2001; **49**:1-70.
31 Berriman M, Ghedin E, Hertz-Fowler C, *et al*. The genome of the African trypanosome *Trypanosoma brucei*. *Science* 2005; **309**:416-422.
32 de Lange T, Borst P. Genomic environment of the expression-linked extra copies of genes for surface antigens of *Trypanosoma brucei* resembles the end of a chromosome. *Nature* 1982; **299**:451-453.
33 Hertz-Fowler C, Figueiredo LM, Quail MA, *et al*. Telomeric expression sites are highly conserved in *Trypanosoma brucei*. *PLoS One* 2008; **3**:e3527.
34 Navarro M, Cross GAM. DNA rearrangements associated with multiple consecutive directed antigenic switches in *Trypanosoma brucei*. *Mol Cell Biol* 1996; **16**:3615-3625.
35 Chaves I, Zomerdijk J, Dirks-Mulder A, Dirks RW, Raap AK, Borst P. Subnuclear localization of the active variant surface glycoprotein gene expression site in *Trypanosoma brucei*. *Proc Natl Acad Sci USA* 1998; **95**:12328-12333.
36 Morrison LJ, Marcello L, McCulloch R. Antigenic variation in the African trypanosome: molecular mechanisms and phenotypic complexity. *Cell Microbiol* 2009; **11**:1724-1734.
37 Holthausen JT, Wyman C, Kanaar R. Regulation of DNA strand exchange in homologous recombination. *DNA Repair (Amst)* 2010; **9**:1264-1272.
38 Proudfoot C, McCulloch R. Distinct roles for two RAD51-related genes in *Trypanosoma brucei* antigenic variation. *Nucleic Acids Res* 2005; **33**:6906-6919.
39 McCulloch R, Barry JD. A role for RAD51 and homologous recombination in *Trypanosoma brucei* antigenic variation. *Genes Dev* 1999; **13**:2875-2888.
40 Hartley CL, McCulloch R. *Trypanosoma brucei* BRCA2 acts in antigenic variation and has undergone a recent expansion in BRC repeat number that is important during homologous recombination. *Mol Microbiol* 2008; **68**:1237-1251.
41 Kim HS, Cross GAM. Identification of *Trypanosoma brucei* RMI1/BLAP75 homologue and its roles in antigenic variation. *PLoS One* 2011; **6**:e25313.
42 Kim HS, Cross GAM. TOPO3alpha influences antigenic variation by monitoring expression-site-associated *VSG* switching in *Trypanosoma brucei*. *PLoS Pathog* 2010; **6**:e1000992.
43 Boothroyd CE, Dreesen O, Leonova T, *et al*. A yeast-endonuclease-generated DNA break induces antigenic switching in *Trypanosoma brucei*. *Nature* 2009; **459**:278-281.
44 Ginger ML, Blundell PA, Lewis AM, Browitt A, Gunzl A, Barry JD. *Ex vivo* and *in vitro* identification of a consensus promoter for *VSG* genes expressed by metacyclic-stage trypanosomes in the tsetse fly. *Eukaryot Cell* 2002; **1**:1000-1009.
45 Yang X, Figueiredo LM, Espinal A, Okubo E, Li B. RAP1 is essential for silencing telomeric variant surface glycoprotein genes in *Trypanosoma brucei*. *Cell* 2009; **137**:99-109.
46 Pandya UM, Sandhu R, Li B. Silencing subtelomeric VSGs by *Trypanosoma brucei* RAP1 at the insect stage involves chromatin structure changes. *Nucleic Acids Res* 2013; **41**:7673-7682.
47 Hovel-Miner GA, Boothroyd CE, Mugnier M, Dreesen O, Cross GAM, Papavasiliou FN. Telomere length affects the frequency and mechanism of antigenic variation in *Trypanosoma brucei*. *PLoS Pathog* 2012; **8**:e1002900.
48 Li B, Espinal A, Cross GAM. Trypanosome telomeres are protected by a homologue of mammalian TRF2. *Mol Cell Biol* 2005; **25**:5011-5021.
49 Chen Y, Yang Y, van Overbeek M, *et al*. A shared docking motif in TRF1 and TRF2 used for differential recruitment of telomeric proteins. *Science* 2008; **319**:1092-1096.
50 Wirtz E, Leal S, Ochatt C, Cross GAM. A tightly regulated

inducible expression system for dominant negative approaches in *Trypanosoma brucei*. *Mol Biochem Parasitol* 1999; **99**:89-101.
51 Takai KK, Kibe T, Donigian JR, Frescas D, de Lange T. Telomere protection by TPP1/POT1 requires tethering to TIN2. *Mol Cell* 2011; **44**:647-659.
52 Kolev NG, Ramey-Butler K, Cross GAM, Ullu E, Tschudi C. Developmental progression to infectivity in *trypanosoma brucei* triggered by an rna-binding protein. *Science* 2012; **338**:1352-1353.
53 Arudchandran A, Bernstein RM, Max EE. Single-stranded DNA breaks adjacent to cytosines occur during Ig gene class switch recombination. *J Immunol* 2004; **173**:3223-3229.
54 Giresi PG, Lieb JD. Isolation of active regulatory elements from eukaryotic chromatin using FAIRE (Formaldehyde Assisted Isolation of Regulatory Elements). *Methods* 2009; **48**:233-239.
55 Glover L, McCulloch R, Horn D. Sequence homology and microhomology dominate chromosomal double-strand break repair in African trypanosomes. *Nucleic Acids Res* 2008; **36**:2608-2618.
56 Riethman H. Human telomere structure and biology. *Annu Rev Genomics Hum Genet* 2008; **9**:1-19.
57 Murnane JP. Telomeres and chromosome instability. *DNA Repair (Amst)* 2006; **5**:1082-1092.
58 Landeira D, Bart JM, Van Tyne D, Navarro M. Cohesin regulates VSG monoallelic expression in trypanosomes. *J Cell Biol* 2009; **186**:243-254.
59 Gunzl A, Bruderer T, Laufer G, *et al*. RNA polymerase I transcribes procyclin genes and variant surface glycoprotein gene expression sites in *Trypanosoma brucei*. *Eukaryot Cell* 2003; **2**:542-551.
60 Figueiredo LM, Cross GAM. Nucleosomes are depleted at the VSG expression site transcribed by RNA polymerase I in African trypanosomes. *Eukaryot Cell* 2010; **9**:148-154.
61 Stanne TM, Rudenko G. Active *VSG* expression sites in *Trypanosoma brucei* are depleted of nucleosomes. *Eukaryot Cell* 2010; **9**:136-147.
62 Chen Q, Ijpma A, Greider CW. Two survivor pathways that allow growth in the absence of telomerase are generated by distinct telomere recombination events. *Mol Cell Biol* 2001; **21**:1819-1827.
63 Kim SH, Davalos AR, Heo SJ, *et al*. Telomere dysfunction and cell survival: roles for distinct TIN2-containing complexes. *J Cell Biol* 2008; **181**:447-460 .
64 Siegel TN, Hekstra DR, Kemp LE, *et al*. Four histone variants mark the boundaries of polycistronic transcription units in *Trypanosoma brucei*. *Genes Dev* 2009; **23**:1063-1076.
65 Vanhamme L, Poelvoorde P, Pays A, Tebabi P, Van Xong H, Pays E. Differential RNA elongation controls the variant surface glycoprotein gene expression sites of *Trypanosoma brucei*. *Mol Microbiol* 2000; **36**:328-340.
66 Wang Z, Morris JC, Drew ME, Englund PT. Inhibition of *Trypanosoma brucei* gene expression by RNA interference using an integratable vector with opposing T7 promoters. *J Biol Chem* 2000; **275**:40174-40179.
67 de Lange T, Shiue L, Myers RM, *et al*. Structure and variability of human chromosome ends. *Mol Cell Biol* 1990; **10**:518-527.

(**Supplementary information** is linked to the online version of the paper on the *Cell Research* website.)